Imaging LDL receptor oligomerization during endocytosis using a co-internalization assay

Peng Zou and **Alice Y. Ting**[*]

Department of Chemistry, Massachusetts Institute of Technology, 77 Massachusetts Avenue, Cambridge, Massachusetts 02139, USA.

Abstract

Methods to probe receptor oligomerization are useful to understand the molecular mechanisms of receptor signaling. Here we report a fluorescence imaging method to determine receptor oligomerization state in living cells during endocytic internalization. The wild-type receptor is co-expressed with an internalization-defective mutant, and the internalization kinetics of each is independently monitored. If the receptor internalizes as an oligomer, then the wild-type and mutant isoforms will mutually influence each others' trafficking properties, causing co-internalization of the mutant, or co-retention of the wild-type at the cell surface. Using this approach, we found that the low density lipoprotein (LDL) receptor internalizes as an oligomer into cells, both in the presence and absence of LDL ligand. The internalization kinetics of the wild-type receptor is not changed by LDL binding. We also found that the oligomerization domain of the LDL receptor is located in its cytoplasmic tail.

The oligomerization state of a cellular receptor can control many aspects of that receptor's function, including its enzymatic activity (1), binding interactions (2), or ion conductance (3). Methods that reveal receptor oligomerization state are therefore crucial to fully understanding receptor-mediated signaling. Existing methods can be divided into two classes – those that require cell lysis and receptor purification, and those that probe receptors in living cells. The first class includes co-immunoprecipitation (4), analytical ultracentrifugation (5), gel-filtration analysis, and electrophoresis (6); the underlying problem, however, is that removal of receptors from their physiological context can artificially disrupt or promote receptor oligomerization. Live-cell methods, such as single molecule photobleaching (3), bimolecular fluorescence complementation (4), fluorescence resonance energy transfer (6), chemical cross-linking (7), and fluorescence recovery after photobleaching (8), circumvent this problem and are likely to be more accurate. One drawback of these methods, however, is that they do not easily distinguish between receptor subpopulations – such as receptor pools undergoing exocytosis versus endocytosis. Since receptor oligomerization can be dynamically regulated in space and time, it would be desirable to have a live-cell method that reveals the oligomerization state of defined receptor subpopulations.

Here we report a new method to determine the oligomerization state of receptors in living cells undergoing endocytosis. We apply the method to analyze the low density lipoprotein receptor (LDL receptor, or LDLR). LDLR is a single-pass transmembrane protein that binds to the LDL particle in serum, internalizes it via clathrin-coated pits, and then releases the LDL in endosomes, before recycling back to the cell surface to bind more LDL particles.

[*]Corresponding author, ating@mit.edu.

Meanwhile, released LDL is targeted to lysosomes for degradation so that its cholesterol content can be extracted for cellular metabolism (9). Due to the central role of LDLR in maintaining cholesterol homeostasis in animals, mutations in this receptor can give rise to diseases such as familial hypercholesterolemia, which afflicts 1 in 500 people (10).

Previous studies have attempted to determine the oligomerization state of LDLR. Chemical cross-linking detected LDLR dimers (7), and electron microscopy revealed LDL dimers on the cell surface and within clathrin-coated pits (11). The former method is not subpopulation-specific, however, and the latter study raises questions of whether ligand-free LDLRs are also dimeric and whether the cell fixation that is required for electron microscopy affects LDLR oligomerization.

Our methodology (Figure 1) is based on assaying for separate or linked behavior of two receptor isoforms that exhibit distinct trafficking properties, but are co-expressed in the same cell. For example, wild-type LDLR can be co-expressed with an internalization-defective mutant LDLR (that fails to target to clathrin-coated pits, for example). If LDLR is monomeric during endocytosis, then we would expect these two isoforms to behave independently: wild-type LDLR internalizes into cells, while mutant LDLR remains on the cell surface (Figure 1c, top row). If, on the other hand, LDLR is oligomeric during endocytosis, then the fates of the two LDLR isoforms will be linked: if wild-type is dominant, then the mutant LDLR will internalize also; if the mutant is dominant, then wild-type LDLR will remain on the cell surface (Figure 1c, middle and bottom rows). Co-internalization or co-retention of the two LDLR isoforms therefore provides evidence of receptor oligomerization. In the case of a negative result, controls must be performed to establish that the receptor mutation(s) disrupt only internalization function and not oligomerization.

Our assay scheme requires monitoring of the internalization properties of one LDLR isoform in the presence of the other isoform. To accomplish this, we used our previously developed biotin ligase (BirA)/streptavidin labeling technique (12). As shown in Figure 1a, a 15-amino acid recognition sequence (the "acceptor peptide" or AP) is fused to the N-terminus of LDLR. This fusion construct is expressed in cells together with endoplasmic reticulum (ER)-targeted BirA (BirA-ER). Using biotin present in the culture medium and ATP naturally present in the ER, BirA-ER site-specifically and covalently biotinylates the AP tag of LDLR. To visualize the cell surface pool of biotinylated AP-LDLR, we simply add fluorophore-conjugated monovalent streptavidin (13) (e.g., mSA-Alexa568) to cells for 2 – 10 minutes, and then wash away unbound excess fluorophore. Because streptavidin is membrane-impermeant, only the surface pool of LDLR is labeled. The use of monovalent streptavidin instead of wild-type streptavidin prevents crosslinking of AP-LDLR (13). Controls in Supplementary Figure 1 show that this labeling scheme is highly specific for AP-LDLR.

Receptor trafficking and oligomerization can be altered by overexpression, so we carefully controlled AP-LDLR expression such that its levels would match those of endogenous LDLR. We also performed recombinant expression in a cell line lacking endogenous LDLR, to avoid complication of our LDLR isoform analysis. Using antibiotic selection, the tetracycline repressor gene was stably integrated into Chinese Hamster Ovary (CHO) cells lacking endogenous LDLR (14) to give T-REx CHO A7 cells. AP-LDLR under a tetracycline-inducible promoter was introduced into these cells using either Lipofectamine 2000 or electroporation. We then titrated the tetracycline concentration to obtain an AP-LDLR expression level comparable to that of endogenous LDLR in wild-type CHO and HeLa cells, as measured by binding to fluorescent LDL (Supplementary Figure 2). These conditions were used for all subsequent experiments.

Due to the size of mSA-Alexa568 (~ 55 kDa), we also checked to see if our labeling would interfere with LDLR function, as measured by LDL binding and uptake into cells. Fluorescent LDL was applied to cells expressing AP-LDLR, either unlabeled or labeled with mSA-Alexa568. We found that both the extent of LDL binding and the extent of LDL uptake after 1 hour incubation were the same in the presence and absence of the mSA-Alexa568 label (Supporting Figure 3).

Using the labeling scheme shown in Figure 1a, we tagged the surface pool of AP-LDLR in T-REx CHO A7 cells with mSA-Alexa568. The cells were then incubated at 37 °C for 5 min to allow endocytosis of labeled receptor. Fluorescent puncta appeared inside the cell (Figure 2a), but conventional fluorescence microscopy does not allow us to distinguish between receptors on the cell surface versus those just inside the cell but near the membrane. We therefore developed a fluorescence quenching strategy to remove cell surface fluorescence and quantify the remaining fluorescence inside the cell. QSY21 is a quencher matched to the wavelength of Alexa568, but when applied as a succinimidyl ester to the cell surface, or as a QSY21-glycine conjugate, we found that the quenching of mSA-Alexa568 fluorescence was incomplete, and water solubility of the reagent was poor. We therefore coupled QSY21 succinimidyl ester to the polyamine spermine, both to improve its water solubility and to enhance electrostatic attraction to the cell surface. This conjugate gave nearly complete quenching of mSA-Alexa568 both in solution (94%, Supplementary Figure 4) and on the surface of mammalian cells (91%, Figure 2a). The same quenching protocol does not affect intracellular fluorescence signal, as shown in separate controls using cells loaded with resorufin fluorophore (Supplementary Figure 5).

Figure 2 shows a QSY quenching experiment using wild-type LDLR. After 5-min incubation at 37 °C, QSY21-spermine was applied to cells expressing AP-LDLR, labeled with mSA-Alexa568. Images were acquired for the same field of view immediately before and after quenching. By calculating the fluorescence intensity ratio for single cells before and after quenching, we could determine the percent of labeled AP-LDLR internalized in a 5-min period. 103 single cells were analyzed, and the distribution of internalization extents was plotted on a histogram. The mean internalization extent was $43.7\% \pm 19.2\%$ (mean $\pm$ s.d.). This value is comparable to previous measurements of LDLR internalization using radioactively-labeled LDL (~ 55% internalization for 5-min incubation) (9).

Next, to perform the complete assay shown in Figure 1c, we required mutants of LDLR with trafficking behavior different from that of wild-type LDLR. Studies of patients with familial hypercholesterolemia have revealed mutants of LDLR that are defective in internalization. Examples of such mutants are shown in Figure 1b. Δ792 LDLR, also called "FH683" (9), is truncated after residue 792 and therefore missing its C-terminal cytoplasmic tail. Y807C and Y807A are point mutants of LDLR with disruptions in the NPxY^{807} motif that is known to be important for receptor targeting to clathrin-coated pits (15). We generated these three LDLR mutants as AP fusions and found that they each indeed exhibit reduced internalization compared to wild-type AP-LDLR in our 5-min assay (Figure 2 and Supplementary Figure 6).

To test for oligomerization, we co-expressed untagged wild-type LDLR with each of the three AP-LDLR mutants in T-REx CHO A7 cells and repeated the above internalization assay. Our analysis shows that there was no increase in internalization for the truncation mutant Δ792 LDLR ($p = 0.71$), whereas both Y807C and Y807A LDLR mutants entered cells more rapidly in the presence of wild-type LDLR than in its absence ($p < 0.001$, Figure 2 and Supplementary Figure 6). We also performed the complementary co-retention assay (Figure 1c, bottom row), co-expressing wild-type AP-LDLR with untagged mutant LDLR. We found that the internalization of the wild-type receptor slowed significantly in the

presence of Y807C LDLR, but not Δ792 LDLR. Separate controls showed that wild-type and mutant LDLRs were efficiently co-expressed in these experiments (untagged receptors could be detected by anti-HA immunofluorescence, Supplementary Figure 7).

These results suggest that the Y807(C/A) LDLR mutants oligomerize with wild-type LDLR, and they mutually affect each others' trafficking: mutant internalization is increased, and wild-type internalization is decreased. In the case of Δ792 LDLR, the region required for LDLR oligomerization may be deleted, and thus co-internalization/co-retention are not possible. Indeed, previous work has suggested that the cytoplasmic domain of LDLR is required for its oligomerization (7). An interesting avenue for future work would be to extend this internalization assay to LDLR mutants with various truncated regions. This would allow us to identify the location of this hypothesized oligomerization domain.

As a negative control, we repeated our analysis using AP-Y807C LDLR co-expressed with the transferrin receptor (TfnR) rather than wild-type LDLR. Like LDLR, the internalization of TfnR proceeds via clathrin-coated pits (16), yet these two receptors do not associate with each other. Enhanced green fluorescent protein (EGFP) was fused to the C-terminus of TfnR to visualize its expression level. As expected, the internalization of AP-Y807C LDLR in the presence of TfnR-EGFP remained low and was uncorrelated with the expression level of TfnR ($R^2 < 0.001$) (Supplementary Figure 8).

We also expressed AP-Δ792 LDLR and AP-Y807C LDLR in wild-type CHO-K1 cells containing endogenous wild-type LDLR. Fluorescence images in Supplementary Figure 9 show that AP-Y807C LDLR was internalized to a greater extent than AP-Δ792 LDLR, in agreement with the above co-expression experiments with wild-type LDLR in T-REx CHO A7 cells (Figure 2).

To test if LDLR oligomerization is affected by LDL binding, we repeated these experiments with LDL added into the medium at saturating concentrations. The same results were obtained, suggesting that LDL binding does not affect receptor oligomerization (Figure 3). This is consistent with previous studies showing that the ApoB-100 protein, which is present in one copy on the surface of each LDL particle, binds to LDLR in a 1:1 molar ratio (17).

Our data also allow us to compare the rate of wild-type LDLR internalization in the presence versus absence of LDL binding. Previous studies using monensin, an ionophore that inhibits receptor recycling, concluded that half of the surface LDLR population internalizes only upon addition of LDL (18). Separate studies using electron microscopy found that LDLR is spontaneously localized to clathrin-coated pits and internalized even in the absence of LDL (19). Our data show that the extent of internalization for wild-type LDLR is the same whether or not it is bound to LDL ($p > 0.4$, Figure 4).

To complement our imaging studies, we also used conventional biochemistry to probe LDLR oligomerization. Wild-type AP-LDLR (AP-WT) was co-expressed with HA-tagged wild-type LDLR (HA-WT) in T-REx CHO A7 cells. BirA-ER was also co-expressed to biotinylate AP. After cell lysis, biotinylated receptor was pulled down using streptavidin-coated magnetic particles. The proteins were eluted and analyzed by anti-HA blot and streptavidin blot. Supplementary Figure 10 shows that pull-down of AP-WT receptor with streptavidin also pulls down HA-WT receptor, consistent with oligomerization. As a negative control, the same experiment was performed with AP-Δ792 mutant LDLR in place of wild-type AP-LDLR. In this case, HA-WT receptor was not co-purified with biotinylated AP-Δ792 LDLR, in agreement with the imaging assays above.

In summary, we have developed a fluorescence imaging assay to probe LDLR oligomerization during endocytosis. Using site-specific protein labeling mediated by biotin

ligase and monovalent streptavidin, as well as cell surface fluorescence quenching with a novel reagent, we quantified LDLR internalization under various conditions. We found that during endocytosis, LDLR is capable of oligomerizing in a ligand-independent manner. This oligomerization is mediated by the receptor's cytoplasmic domain. LDLR dimerization was suggested in previous electron microscopy studies and chemical cross-linking experiments but has never been observed directly in live cells, free of potential artifacts from cell lysis and fixation.

An important feature of our assay is that it does not require the use of LDL ligand, making it possible to study receptor oligomerization in both ligand-bound and ligand-free states. Recently, a related strategy called RASSL (receptor activated solely by a synthetic ligand) (20) has been applied to study the co-internalization of mutant and wild-type β_2-adrenergic receptor (21). In comparison, our method does not require chemical synthesis of selective ligands and avoids receptor activation.

On the other hand, a drawback of our method is the need for internalization-defective receptor mutants. For some receptors, such mutants may not be known, or the mutations may disrupt receptor oligomerization or other aspects of receptor function. A final caveat is that receptors may associate with each other indirectly, via an intermediate scaffolding protein for example. In this case, rather than revealing direct physical contacts between receptor monomers, the observed co-internalization and/or co-retention could indicate that these monomers are embedded in a higher-order macromolecular complex. To test this alternative hypothesis for a given scaffolding protein, we could measure the correlation between its expression level (either increased by over-expression or decreased by RNA interference) and the extent of linked behavior of receptor isoforms. A positive correlation would imply that this scaffolding protein might play a role in mediating receptor-receptor association in a cluster.

METHODS

Receptor co-internalization assay

Chinese Hamster Ovary (CHO) cells lacking endogenous LDLR and stably expressing the tetracycline repressor (T-REx CHO A7 cells) were transfected with biotin ligase targeted to the endoplasmic reticulum (BirA-ER), a nuclear YFP transfection marker (H2B-YFP), and wild-type and/or mutant LDLR (differentially tagged with either the acceptor peptide (AP) or HA epitope, as indicated in each figure), using Lipofectamine 2000 (Invitrogen) or Nucleofector (Amaxa). The cells were cultured in 50 ng/mL tetracycline to give LDLR expression levels comparable to endogenous LDLR levels (Supplementary Figure 2). 24 – 36 hours following transfection, the cells were labeled with 80 nM mSA-Alexa568 at 4 °C for 10 min and then rinsed twice with Dulbecco's phosphate buffered saline (DPBS) pre-warmed to 37 °C. Cells were then incubated at 37 °C for 5 min. Following incubation, cells were chilled with ice-cold DPBS and imaged as described in the Supporting Information under "General Methods". To quantify the internalization extent of mSA-labeled receptor, the buffer was aspirated from the imaging dish and ~500 µL of 40 µM QSY21-spermine solution in ice-cold DPBS was added to cover the monolayer of cells. Within 1 min after quenching, fluorescence and DIC images were taken again for cells in the same field of view. To assess the effect of LDL on receptor internalization (Figure 3), 100 µg mL^{-1} LDL was added to the buffer during mSA-Alexa568 labeling, and cells were incubated at 37 °C in the presence of 10 µg mL^{-1} LDL. Details in preparation of mSA-Alexa568 and QSY21-spermine reagents were described in the Supporting Information under "Specific Methods".

Quantitation of receptor internalization

Image analysis was performed using Slidebook 4.2 software. To quantify internalization, a mask for each labeled cell was individually created based on Alexa568 signal in the pre-quench image, and then these masks were copied to the corresponding post-quench (+QSY) image. Occasionally, stage drift caused a shift of a few pixels between images taken before and after quenching, and this was corrected manually by shifting the masks. After subtracting background in the Alexa568 channel, the percent of labeled receptor internalized was calculated for each mask by taking the ratio of fluorescence intensities before and after quenching. The frequency distributions of internalization extent for two data sets were compared using the two-sample Kolmogorov-Smirnov test, and the *p*-values were reported.

Supplementary Material

Refer to Web version on PubMed Central for supplementary material.

Acknowledgments

REFERENCES

1. Schlessinger J. Ligand-induced, receptor-mediated dimerization and activation of EGF receptor. Cell. 2002; 110:669–672. [PubMed: 12297041]

2. Shi YG, Massague J. Mechanisms of TGF-β signaling from cell membrane to the nucleus. Cell. 2003; 113:685–700. [PubMed: 12809600]

3. Ulbrich MH, Isacoff EY. Subunit counting in membrane-bound proteins. Nat. Methods. 2007; 4:319–321. [PubMed: 17369835]

4. Makarova A, Bercury KK, Adams KW, Joyner D, Deng MH, Spoelgen R, Koker M, Strickland DK, Hyman BT. The LDL receptor-related protein can form homo-dimers in neuronal cells. Neurosci. Lett. 2008; 442:91–95. [PubMed: 18602448]

5. Brown PH, Schuck P. Macromolecular size-and-shape distributions by sedimentation velocity analytical ultracentrifugation. Biophys. J. 2006; 90:4651–4661. [PubMed: 16565040]

6. Bouvier M. Oligomerization of G-protein-coupled transmitter receptors. Nat. Rev. Neurosci. 2001; 2:274–286. [PubMed: 11283750]

7. van Driel IR, Davis CG, Goldstein JL, Brown MS. Self-Association of the Low Density Lipoprotein Receptor Mediated by the Cytoplasmic Domain. J. Biol. Chem. 1987; 262:16127–16134. [PubMed: 3680245]

8. Dorsch S, Klotz KN, Engelhardt S, Lohse MJ, Bunemann M. Analysis of receptor oligomerization by FRAP microscopy. Nat. Methods. 2009; 6:225–230. [PubMed: 19234451]

9. Brown MS, Goldstein JL. A Receptor-Mediated Pathway for Cholesterol Homeostasis. Science. 1986; 232:34–47. [PubMed: 3513311]

10. Rader DJ, Cohen J, Hobbs HH. Monogenic hypercholesterolemia: new insights in pathogenesis and treatment. J. Clin. Invest. 2003; 111:1795–1803. [PubMed: 12813012]

11. Heuser JE, Anderson RGW. Hypertonic Media Inhibit Receptor-Mediated Endocytosis by Blocking Clathrin-Coated Pit Formation. J. Cell Biol. 1989; 108:389–400. [PubMed: 2563728]

12. Howarth M, Ting AY. Imaging proteins in live mammalian cells with biotin ligase and monovalent streptavidin. Nat. Protocols. 2008; 3:534–545.

13. Howarth M, Chinnapen DJF, Gerrow K, Dorrestein PC, Grandy MR, Kelleher NL, El Husseini A, Ting AY. A monovalent streptavidin with a single femtomolar biotin binding site. Nat. Methods. 2006; 3:267–273. [PubMed: 16554831]

14. Sege RD, Kozarsky K, Nelson DL, Krieger M. Expression and Regulation of Human Low-Density Lipoprotein Receptors in Chinese Hamster Ovary Cells. Nature. 1984; 307:742–745. [PubMed: 6321999]

15. Chen WJ, Goldstein JL, Brown MS. NPXY, A Sequence Often Found in Cytoplasmic Tails, Is Required for Coated Pit-Mediated Internalization of the Low Density Lipoprotein Receptor. J. Biol. Chem. 1990; 265:3116–3123. [PubMed: 1968060]

16. Iacopetta BJ, Rothenberger S, Kuhn LC. A Role for the Cytoplasmic Domain in Transferrin Receptor Sorting and Coated Pit Formation During Endocytosis. Cell. 1988; 54:485–489. [PubMed: 2900073]

17. Jeon H, Blacklow SC. Structure and physiologic function of the low-density lipoprotein receptor. Ann. Rev. Biochem. 2005; 74:535–562. [PubMed: 15952897]

18. Basu SK, Goldstein JL, Anderson RGW, Brown MS. Monensin Interrupts the Recycling of Low Density Lipoprotein Receptors in Human Fibroblasts. Cell. 1981; 24:493–502. [PubMed: 6263497]

19. Brown MS, Anderson RGW, Goldstein JL. Recycling Receptors: the Round-Trip Itinerary of Migrant Membrane-Proteins. Cell. 1983; 32:663–667. [PubMed: 6299572]

20. Coward P, Wada HG, Falk MS, Chan SDH, Meng F, Akil H, Conklin BR. Controlling signaling with a specifically designed G_i-coupled receptor. Proc. Natl. Acad. Sci. U. S. A. 1998; 95:352–357. [PubMed: 9419379]

21. Sartania N, Appelbe S, Pediani JD, Milligan G. Agonist occupancy of a single monomeric element is sufficient to cause internalization of the dimeric β_2–adrenoceptor. Cell. Signal. 2007; 19:1928–1938. [PubMed: 17561373]
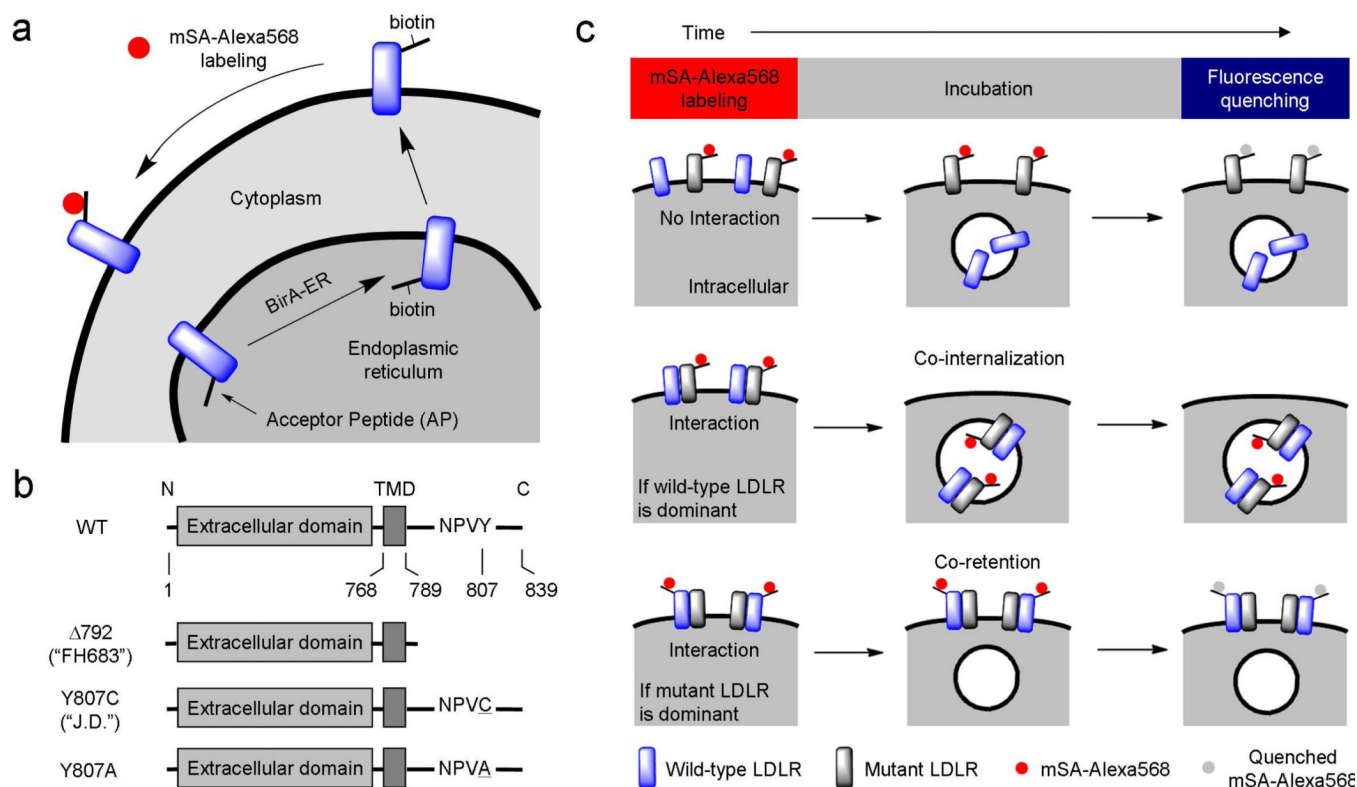
Figure 1.
Fluorescence labeling and imaging assay to probe receptor oligomerization state. a) Site-specific biotinylation of "acceptor peptide" (AP)-fused receptors with biotin ligase (BirAER), and surface labeling with AlexaFluor568-conjugated monovalent streptavidin (mSA) (12). b) Domain structures of wild-type (WT) and internalization-defective mutants of the low density lipoprotein receptor (LDLR). The NPVY sequence in the cytoplasmic tail is responsible for targeting to clathrin-coated pits (15). TMD = transmembrane domain. c) Scheme for oligomerization assay. Cells co-expressing wild-type LDLR and AP-tagged mutant LDLR are labeled with mSA-Alexa568 and then incubated at 37 °C to allow receptor internalization. The extent of internalization is quantified by single-cell imaging after quenching of surface fluorescence with QSY21-spermine. If LDLR internalizes as a monomer, then mutant LDLR will remain on the cell surface, while wild-type LDLR separately internalizes (first row). If, on the other hand, LDLR is oligomeric during internalization, then mutant LDLR might co-internalize along with wild-type LDLR (second row), or wild-type LDLR might be co-retained at the cell surface with mutant LDLR (third row). In this final scheme (third row), wild-type LDLR is tagged with AP rather than mutant LDLR.
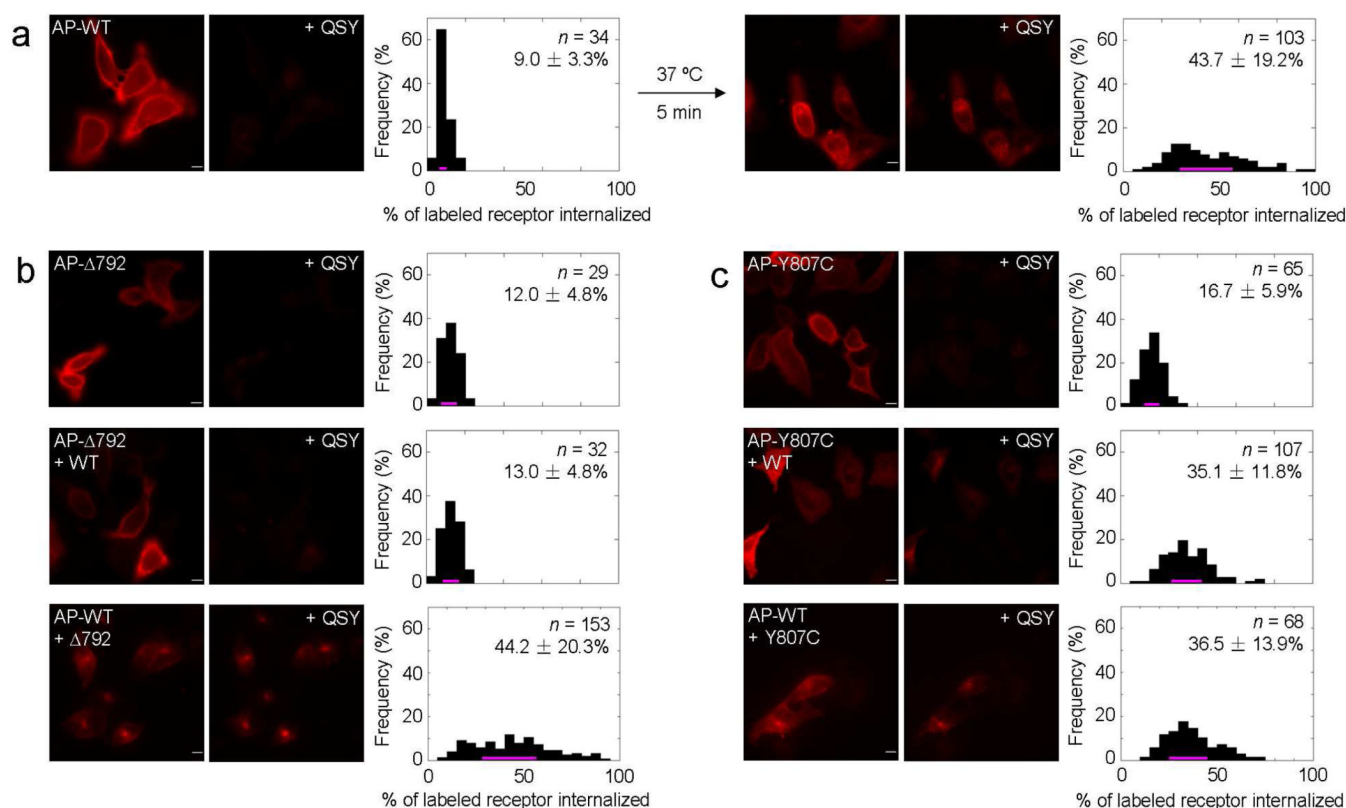
Figure 2.
Analysis of LDLR oligomerization in the absence of LDL. T-REx CHO A7 cells (lacking endogenous LDLR) expressing BirA-ER and the indicated LDLR construct(s) were labeled with mSA-Alexa568. Representative images are shown immediately before and after surface fluorescence quenching with QSY21-spermine (+QSY). Percent of internalized AP-receptor was quantified for single cells, and the distributions of these percentages are shown in histograms, with pink lines denoting the interquartile ranges (25–75%). Means are shown ± s.d. a) Internalization analysis of AP-tagged wild-type LDLR (AP-WT), after 0 min (left) and 5 min (right) incubation at 37 °C. Some internalized receptor is seen at 0 min due to background internalization during mSA-Alexa568 labeling and image acquisition. After 5 min incubation, more Alexa568 fluorescence is protected from QSY quenching, indicating receptor internalization. b) Same analysis for the Δ792 mutant of LDLR (AP-Δ792). Images are shown ±QSY quenching after 5 min incubation at 37 °C. In the second row, untagged wild-type LDLR (WT) is co-expressed. In the third row, Δ792 LDLR and wild-type LDLR are again co-expressed, but the AP tag is on wild-type LDLR instead. c) Same as b) but using the Y807C mutant of LDLR. Scale bars = 10 µm. Data for the Y807A mutant of LDLR are shown in Supplementary Figure 6.
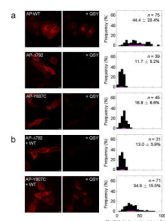
Figure 3.
Analysis of LDLR oligomerization in the presence of LDL. T-REx CHO A7 cells expressing BirA-ER and the indicated LDLR construct(s) were labeled with mSA-Alexa568 in the presence of 100 µg/mL LDL, and then incubated at 37 °C for 5 min with 10 µg/mL LDL. Fluorescence quenching with QSY21-spermine, imaging, and internalization analysis were performed as in Figure 2. a) Analysis of cells expressing wild-type LDLR (AP-WT) or mutant LDLR alone. b) Analysis of cells co-expressing wild-type LDLR and AP-tagged mutant LDLR. Scale bars = 10 µm.
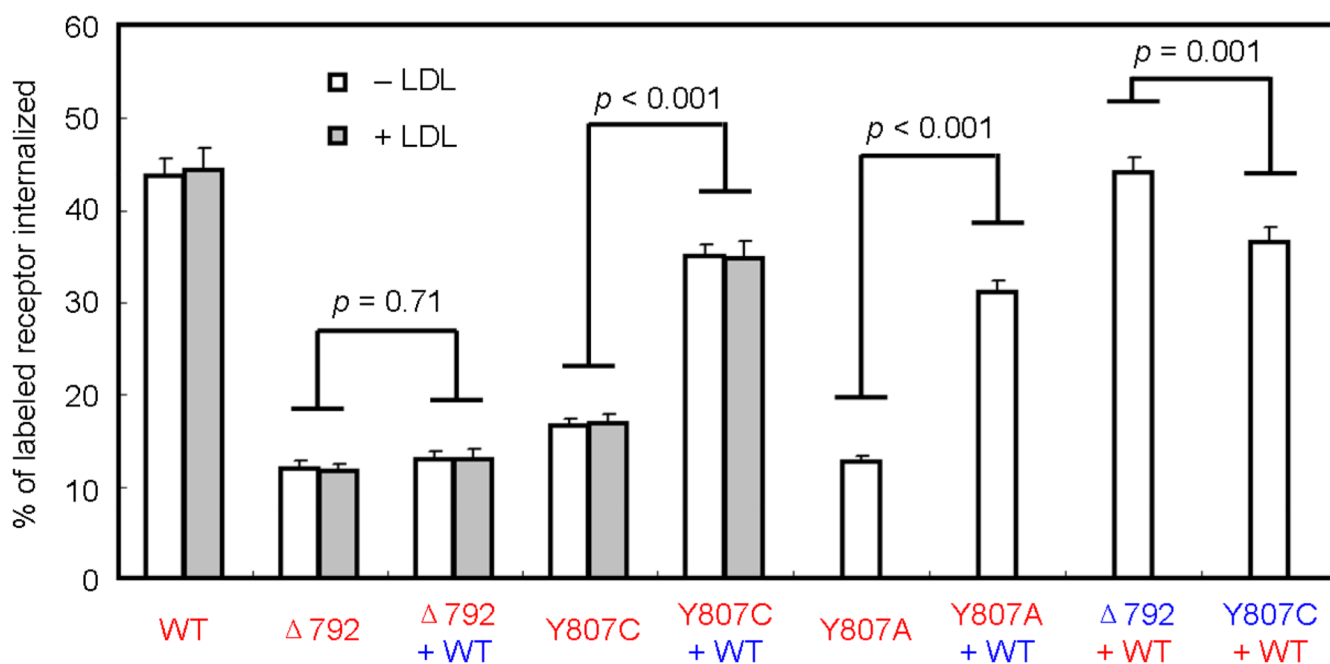
Figure 4.
Summary of oligomerization assay data from Figures 2–3 and Supplementary Figure 6. The AP-tagged receptor is shown in red; unlabeled receptors are in blue font. The presence of LDL does not affect receptor internalization ($p > 0.4$, Kolmogorov-Smirnov test). Unlike the truncation mutant Δ792, the internalization of Y807C and Y807A mutants increase significantly when co-expressed with wild-type LDLR. Meanwhile, the internalization of wild-type LDLR is reduced when it is co-expressed with Y807C, but not Δ792 LDLR ($p = 0.001$). Data are given as mean ± s.e.m.